Modulating functional connectivity after stroke with neurofeedback: Effect on motor deficits in a controlled cross-over study

Anaïs Mottaz, Tiffany Corbet, Naz Doganci, Cécile Magnin, Pierre Nicolo, Armin Schnider, Adrian G. Guggisberg*

Division of Neurorehabilitation, Department of Clinical Neurosciences, University Hospitals Geneva, Avenue de Beau-Séjour 26, 1211 Geneva, Switzerland

ARTICLE INFO

ABSTRACT

Synchronization of neural activity as measured with functional connectivity (FC) is increasingly used to study the neural basis of brain disease and to develop new treatment targets. However, solid evidence for a causal role of FC in disease and therapy is lacking. Here, we manipulated FC of the ipsilesional primary motor cortex in ten chronic human stroke patients through brain-computer interface technology with visual neurofeedback. We conducted a double-blind controlled crossover study to test whether manipulation of FC through neurofeedback had a behavioral effect on motor performance. Patients succeeded in increasing FC in the motor cortex. This led to improvement in motor function that was significantly greater than during neurofeedback training of a control brain area and proportional to the degree of FC enhancement. This result provides evidence that FC has a causal role in neurological function and that it can be effectively targeted with therapy.

1. Introduction

Interregional neural communication is thought to be accompanied by a synchronization of oscillations between different brain regions (Fries, 2005; Varela et al., 2001). This interregional synchronization can be quantified with the concept of *functional connectivity (FC),* which is a measure of statistical dependency between activities in different brain areas. The human brain maintains an organized pattern of interregional synchronization even during periods without externally given task (Damoiseaux et al., 2006; Greicius et al., 2003; Vincent et al., 2007) and FC can be observed from recordings of neural oscillations at several frequency bands (Deriche, 2016; Guggisberg et al., 2015).

Analyses of FC are convenient and now abundantly used to probe for novel disease biomarkers (Fox and Greicius, 2010), treatment targets (Zhang et al., 2016), or predictors of outcome (Nicolo et al., 2015; Westlake et al., 2012). However, in contrast to the frequent usage of this approach, it is currently justified only by correlations in observational imaging studies. The strength of FC during a task-free state correlates with behavioral performance in a variety of cognitive and motor functions in healthy humans (Guggisberg et al., 2015; Hampson et al., 2006; Hipp et al., 2011; Schlee et al., 2012). Furthermore, several brain pathologies and neurological deficits are associated with disruptions of FC among networks (Baldassarre et al., 2016; Carter et al., 2010;

Dubovik et al., 2012; Fellrath et al., 2016; He et al., 2007). There are also studies suggesting a functional significance of FC in learning. Motor, perceptual, and phonological learning as well as memory tasks specifically modulate FC during (Sun et al., 2007) and after the tasks (Albert et al., 2009; Sami et al., 2014; Tambini et al., 2010; Veroude et al., 2010).These FC changes correlate with the degree of learning (Lewis et al., 2009; Tambini et al., 2010).

However, FC networks during resting state are only weakly correlated to networks during tasks (Davis et al., 2017; Rehme et al., 2013). Furthermore, correlations between neural and behavioral traits do not necessarily imply a causal relationship. More decisive evidence concerning causality would therefore be needed before we can apply FC techniques to clinical questions. One way to achieve this is by manipulating specific FC patterns while assessing the effect on behavioral measures (Poldrack and Farah, 2015).

Here, we propose to use the method of neurofeedback to induce FC enhancements in motor networks in human stroke patients and test the resulting impact on clinical deficits. Neurofeedback enables the monitoring of brain activity and the generation of a real-time output about specific changes in activity patterns. The recorded subject can thus learn to voluntarily modulate his own brain function. The crucial advantage of this approach is that it enables us to selectively manipulate a specific pattern of neural activity, including FC (Bassett and Khambhati,

---

2017; Liew et al., 2016; Mottaz et al., 2015; Ramot et al., 2017; Sacchet et al., 2012). Recent pioneering studies have shown that FC enhancement with neurofeedback can produce subjective emotional changes (Koush et al., 2017) and improve bimanual finger tapping (Kajal et al., 2017) of healthy subjects. Here we report the first double-blind controlled clinical trial in a stroke patient population in order to further demonstrate a causal link between network communication and brain disease.

We previously observed that the magnitude of alpha-band FC is correlated with behavioral performance in stroke patients. The more the ipsilesional primary motor cortex remained coherent with the rest of the brain, as reflected by a higher weighted node degree, the better patients were able to move their arms and the less severe was their hemiparesis (Dubovik et al., 2012). We therefore trained chronic stroke patients to enhance the weighted node degree of structurally preserved areas in their ipsilesional primary motor cortex and measured the effect on motor performance. In a control condition, patients performed neurofeedback training of the weighted node degree at a brain area that is implicated in higher level function and that did not correlate with motor performance in chronic stroke patients, using a double-blind cross-over design. Our hypothesis was that training weighted node degree of the primary motor cortex would be associated with a better motor function improvement than training the control region and that the improvement would be proportional to the degree of success in coherence training.

2. Materials and methods

2.1. Participants

Thirteen stroke patients gave written informed consent and the Ethics Committee of the Canton of Geneva approved the study. Inclusion criteria were the presence of ischemic or hemorrhagic stroke in chronic stage (at least 9 months after onset) and unilateral deficits in upper limb motor function with significant impact on daily activities. Exclusion criteria were the inability to participate in long treatment sessions, inability to concentrate for prolonged periods, metallic objects in the brain, presence of implants or neural stimulators, persistent delirium or disturbed vigilance, moderate or severe language comprehension deficits, new stroke lesions during treatment, and medical complications. Demographic and clinical characteristics of patients are shown in Table 1. Two patients had to be excluded because of medical complications unrelated to the study procedures and one patient withdrew from the study. Among the ten patients who completed the study, five were females and all participants were right-handed. Their

mean age was 57.1 years old (range 40–71 years). They had been diagnosed with unilateral, territorial, ischemic (six patients) or hemorrhagic stroke (four patients) in the territories of the middle cerebral artery. Five patients had a purely subcortical lesion while the other five had a mixed cortical-subcortical lesion. Patients were between eleven months and five years post-stroke (mean 2.6 years) and had moderate to severe upper limb motor impairment (mean Fugl-Meyer score 26/66 points, range 15–54) (Table 1).

The study was registered with ClinicalTrials.gov, identifier NCT02223910.

2.2. Structural MRI and lesion mapping

The MRI protocol contained a high-resolution T1-weighted, 3-D spoiled gradient-recalled echo in a steady state sequence covering the whole skull (192 coronal slices, 1.1 mm thickness, TR = 2500 ms, TE = 3 ms, flip angle = 8°), T2-weighted three-dimensional fast spin-echo and diffusion weighed imaging sequences with 30 diffusion encoding directions (slice resolution of 2 mm) performed on a 3 T Siemens Siemens Trio TIM scanner (Siemens Medical Solutions, Erlangen, Germany). Damaged regions were delineated directly as volume of interest (VOI) on the axial diffusion-weighted MRI scans, resliced and aligned to T1 using SPM8 (www.fil.ion.ucl.ac.uk/spm). Lesion maps were normalized to MNI (http://www.bic.mni.mcgill.ca) space using SPM8. A lesion mask was used to reduce the contribution of damaged tissue during normalization (Brett et al., 2001). Degree of internal capsule damage was estimated using the JHU White Matter atlas and normalized lesion masks by dividing voxels in common between both masks by the size of the internal capsule mask.

2.3. Neurofeedback

2.3.1. Target areas

Patients learned to enhance an FC pattern that correlates with performance in stroke patients (Dubovik et al., 2012). In the active treatment period, they aimed at training the weighted node degree, i.e., the sum of FC between the ipsilesional hand motor cortex area and the rest of the brain. The region was defined with radius of 20 mm centered on the hand knob. Areas with structural damage were excluded. For the control period, the weighted node degree of the contralesional rostrolateral prefrontal cortex around MNI coordinates x = 30, y = 45, z = 25 (Brodmann area 10) was used for feedback. The usage of a control area with real feedback gave us a more stringent control of unspecific effects than random pseudo-feedback that is typically used in neurofeedback trials. Patients had the possibility of developing actual

Table 1
Patient characteristics.

Patient	Age	Gender	Handedness	Side of motor deficit	Stroke aetiology	Stroke Type	Lesion Type	Lesion Volume	Time since stroke (months)	NIH stroke scale at admission	Baseline Fugl-Meyer score (UE)
P1	57	F	R	L	Primary CNS vasculitis	I	Mixed	75	61	11	23
P2	52	F	R	R	Cryptogenic	I	Subcortical	80	53	27	17
P4	40	M	R	R	Arterial hypertension	H	Mixed	23	27	21	22
P5	65	M	R	L	Arterial hypertension	H	Subcortical	52	14	17	17
P6	65	F	R	R	Cryptogenic	H	Mixed	46	53	9	46
P8	55	M	R	L	Arterial hypertension	H	Subcortical	75	14	15	15
P10	52	F	R	R	Cryptogenic	H	Mixed	52	17	13	18
P11	62	M	R	L	Arterio-arterial embolism	I	Subcortical	51	11	17	19
P12	71	M	R	R	Arterio-arterial embolism	I	Subcortical	8	37	8	54
P13	52	F	R	L	Cryptogenic	I	Mixed	304	15	14	29

Abbreviations: F = female, M = male, R = right, L = left, I = ischemic, H = hemorrhagic.

control over their brain activity in both conditions. This allowed us to test for spatial specificity of the intervention. While the prefrontal cortex may have a role in motor function and learning (Rehme et al., 2013; Sharma et al., 2009), it is implicated in high-level functions spanning many domains (Ramnani and Owen, 2004). We hypothesized that the training of the global FC of this region would have a limited impact on motor recovery, supported by the absence of correlation between its weighted node degree and motor performance (Dubovik et al., 2012).

2.3.2. Task

Patients received visual feedback on their current alpha-band (8–12 Hz) node degree in the target area on a computer screen in front of them. Feedback was composed of a vertical scale made of 12 white horizontal bars, over a black background, representing from bottom to top, low to high alpha-band node degree values. Every 300 ms, the bar with the value closest to the currently calculated node degree value was highlighted in blue. The highest bar reached during the current trial was constantly highlighted in green and updated when necessary. During 45 s, subjects tried to raise the bars as high as possible. If the current value reached the top of the scale, the trial continued normally until the end of the 45 s with no specific visual reward other than the top bar highlighted in green. No particular strategy was proposed (Mottaz et al., 2015). We told patients not to physically move their upper limbs and keep the eyes opened. To avoid frustration, the scale of the feedback was adapted for each participant between and within sessions, such that his or her FC values were within reach of the top bar, as estimated visually. The scale was most of the time set between −2.5 and + 2.5 standard deviations of FC z-score.

2.3.3. Study design

Patients were alternatively assigned to start with either the motor cortex FC training or the control region FC training. Each arm of training was composed of eight sessions, two per week, distributed over one month. To avoid a carry-over effect, a wash-out period of one month without neurofeedback between control and motor training was established. Each neurofeedback session was preceded by a 30 min active upper limb motor training with a trained physical therapist, who was blinded for the type of training period (motor or control), in order to potentiate the effect of the neurofeedback. A neurofeedback session began with an EEG recording of 10 min in a resting-state condition with eyes closed. Neurofeedback training itself lasted 50 min and consisted of 50 neurofeedback trials of 45 s each with longer pauses every five minutes.

2.3.4. Data acquisition

EEG data were acquired with a 128-channel BioSemi ActiveTwo EEG-system (BioSemi B.V., Amsterdam, Netherlands) at a sampling rate of 512 Hz. Electrodes containing electrode or muscle artefacts or abundant noise were selected through visual inspection at the beginning of each session and every five minutes during pauses and rejected from further analysis. During neurofeedback, the incoming data stream was continuously written into a FieldTrip buffer (Oostenveld et al., 2011) and simultaneously recorded for offline analysis. The last 500 ms data segment was read every 300 ms in MATLAB (R2011a, The Math-Works inc., Natick, USA) using the FieldTrip toolbox (http://www.fieldtriptoolbox.org). The data segment was bandpass filtered between 1 and 20 Hz with a 4th-order butterworth filter. Data windows with mean channel variance exceeding 90% of what was observed during first resting-state of session were discarded to remove segments with artefacts.

In contrast to classical neurofeedback studies for motor function, patients in the present trial did not train to enhance activation of the motor cortex, but to increase a resting-state correlate of motor performance. Motor imagery does not lead to an increase of alpha-band co-herence between motor cortex and the rest of the brain (Mottaz et al.,

2015). In order to further exclude EMG confounders, we used two approaches. First, we systematically questioned patients on their strategy used. Second, muscle activity of the hemiparetic forearm was monitored with electromyography in the first two patients. Active electrodes were placed on the belly of the abductor pollicis and of the extensor carpi radialis.

2.3.5. Source signal reconstruction

Realistic head geometry was used for the forward problem estimation with the Boundary Element Method (BEM) based on the segmented grey matter of individual T1 MRI. Electrode positions were recorded and digitized with a Polhemus Fastrak system (Colchester, USA) and co-registered to the individual MRI. The BEM model was created with the open source Matlab toolbox NUTMEG (http://www.nitrc.org/plugins/mwiki/index.php/nutmeg:MainPage) (Dalal et al., 2011) using the Helsinki BEM library (http://peili.hut.fi/BEM/) (Stenroos et al., 2007). Solution points were defined using a 10 mm grid spacing (~1000 solution points). The signal was then projected to the grey-matter voxels with a minimum variance beamformer method, an adaptive spatial filter optimized on data covariance. Computation of the spatial filter w used the column-normalized lead-potential L as well as the channel covariance R obtained from the first resting-state recording of each session in 7 patients and from the immediately preceding feedback block of the current session in 3 patients:

$$\mathbf{w}(r) = \frac{\mathbf{R}^{-1}\mathbf{L}(r)}{\mathbf{L}^{\mathrm{T}}(r)\mathbf{R}^{-1}\mathbf{L}(r)},$$

where r represents each solution point. Dipole orientations were fixed so that they yielded maximum output signal-to-noise ratio at each solution point (Sekihara et al., 2004).

2.3.6. Real-time functional connectivity

Functional connectivity was quantified using the absolute imaginary part of coherency (IC) (Nolte et al., 2004), a spectral measure of FC that ignores zero-phase-lag coherence. The advantage of IC over other measures of FC is that it is not subject to biases arising from volume conduction or spatial leakage of the inverse solution (Sekihara et al., 2011). Although the spatial resolution of EEG souce imaging is imperfect, the usage of IC with inverse solutions and realistic head models provides sufficient spatial resolution for demonstrating training effects in ipsilesional motor areas compared to control areas in other lobes.

IC was calculated by tapering 500 ms epochs with a Hann window and performing a discrete Fourier transform with 512 frequency bins at all electrodes. The complex Fourier coefficients F at all electrodes were projected into source space with the adaptive spatial filter:

$$G(f) = \mathrm{W}^{\mathrm{T}}F(f)$$

where T indicates the matrix transpose. Complex coherency was computed from the Fourier transformed source time series G from each voxel to all other voxels resulting in a full all-to-all voxel complex connectivity matrix C:

$$C(f) = \frac{G(f) * G(f)}{\sqrt{diag(|G(f)|^{T}|G(f)|)\, diag(|G(f)|^{T}|G(f)|)^{T}}}$$

where * denotes the complex conjugate and diag(M) the vector formed by the diagonal entries of the matrix M. Complex coherency at the alpha band was obtained by summing the cross- and auto-spectra across the corresponding frequency bins between 8 and 12 Hz. IC was finally obtained after variance-stabilizing Fisher's Z transform:

$$IC(f) = \left| \mathrm{Im}\, \frac{C(f)}{|C(f)|} \arctan h(|C(f)|) \right|$$

where Im is the imaginary component and arctanh the inverse hyperbolic tangent.

To obtain a more stable feedback, current alpha-band IC was

averaged over the last 12 overlapping segments (last 3.8 s) using a sliding window.

The weighted node degree was then computed. Nodes were defined as individual voxels d edges between all pairs of voxels were weighted by IC values. Node degree, corresponding to the number of edges incident to a node, was extended to the sum of weight and referred as weighted node degree (Newman, 2004). The weighted node degree k of each voxel i was calculated as the sum of its IC with all other voxels j:

$$k_i = \sum_i \text{IC}_{ij}$$

It can be seen as an index of the overall importance of an area in the brain network (Stam and van Straaten, 2012). To minimize the potential confound of changes in signal-to-noise ratio influencing IC magnitude, we normalized weighted node degrees by calculating z-scores (Dubovik et al., 2012). This was achieved by subtracting the mean weighted node degree of all voxels from the values at target voxels and dividing by the standard deviation over all voxels. The mean normalized weighted node degree of voxels in the target region was then used for visual feedback. Mean computation time was < 250 ms. Feedback was updated every 300 ms.

2.4. Clinical assessment

The effect of neurofeedback training on motor performance was assessed by a trained physical therapist who was blinded for the type of training period (motor or control). Evaluations were obtained before the first training session, after the last training session, and one month after the end of each training period. For one patient, no long-term follow-up evaluation of motor performance could be obtained for the second treatment period due to patient refusal.

A single primary outcome measure was prespecified at ClinicalTrials.gov, identifier NCT02223910: the upper limb Fugl-Meyer motor assessment with a maximal score of 66 points (Fugl-Meyer et al., 1975; Gladstone et al., 2002). Secondary measures included the Nine Hole Peg test (Kellor et al., 1971) as well as the Box and Block test for dexterity assessment (Lin et al., 2010; Mathiowetz et al., 1985). Upper extremity muscle strength was evaluated with the Medical Research Council muscle scale (Compston, 2010) and grip strength was evaluated with a Jamar dynamometer (Schmidt and Toews, 1970). The impact on daily living tasks was evaluated with the Motor Activity Log–14 score (Uswatte et al., 2005). The 10 Meter Walk (Perera et al., 2006) and the Time Up and Go test (Flansbjer et al., 2005) were used to measure the more global impact on functional mobility and lower extremity motor performance. The European Stroke Scale was used for a global clinical assessment (Hantson et al., 1994). Spasticity was evaluated with the modified Ashworth scale (Bohannon and Smith, 1987).

2.5. Statistical analyses

All analyses were made using MATLAB (R2011a, The MathWorks inc., Natick, USA). Normality was determined with Shapiro-Wilk or Shapiro-Francia tests depending on the shape of the data.

2.5.1. Clinical effect

Statistical assessments were made with parametric Student t-test and non-parametric Wilcoxon signed ranked test for data showing normal and non-normal distribution respectively.

2.5.2. Offline functional connectivity

We assessed the neural effect of neurofeedback training by investigating the change in alpha-band (8–12 Hz) weighted node degree over time. The signal recorded during the neurofeedback sessions was divided into five blocks each representing ten minutes of neurofeedback training. A value of alpha-band weighted node degree was calculated for each block. The change in alpha weighted node degree during the

neurofeedback session was estimated at each voxel by computing the linear regression (least-square minimization) coefficient, or slope, using the five node degree values, modeling the relationship between time and alpha weighted node degree. The regression coefficient represented the estimated change during 10 min of neurofeedback. For each block, the calculation of the alpha weighted node degree was identical to the method used during the neurofeedback, described in Section 2.3.6 except the following differences: the data were splitted into 1000 ms data segments, bad electrodes were excluded through automatic detection based on amplitude correlation with neighbours and mean variance and through visual inspection, segments with artefacts were excluded through visual inspection and automatic detection based on deviation from channel mean, global variance and amplitude difference between minimal and maximal values. The adaptive spatial filter was computed using data covariance from the neurofeedback data themselves. The mean weighted node degree slope across voxels in the defined target area of all patients was subjected to parametric Student t-test (given normally distributed values) testing the null hypothesis of zero slope.

To visualize the spatial specificity of these changes, we additionally obtained voxel-wise assessments of the average slope of the eight sessions. Maps of average slopes were spatially normalized to canonical MNI space and flipped along the midsagittal plane in subjects who trained the right motor cortex. Statistical non-parametric mapping (SnPM) assessed the statistical significance of the increase in FC at each voxel via permutations with random reversions of the original data (Singh et al., 2003). Since we were interested in visualizing the full extent of FC increases to confirm spatial specificity, we did not correct for testing multiple voxels in this analysis. This produced a whole brain map of the voxels with a significant increase or decrease in FC during the neurofeedback sessions.

To visualize the pattern of FC increase between the motor target area and the other regions of the brain, a whole brain map was created by computing the seed-based FC slope between each voxel and the motor target voxels, statistically assessed with SnPM.

To test for changes in resting-state FC in the absence of feedback, we also computed the linear regression (least-square minimization) slope over the eight resting-state recordings obtained before each neurofeedback session, hence quantifying the evolution of the weighted node degree in the alpha-band over the month of training. The alpha-band weighted node degree of each resting–state recording was computed from five minutes of artefact-free data and as described above.

2.5.3. Power

Power evolution in the alpha-band during neurofeedback session was estimated analogously by computing the linear regression slope over five blocks, each representing ten minutes of neurofeedback training, using the same preprocessed data as for functional connectivity analysis. Slopes of z-normalized power were tested voxel-wise for significance with SnPM, and in the defined target area with parametric Student t-test (given normally distributed values).

2.5.4. Electromyography

We evaluated the muscle activity by calculating the root mean square of the highpass filtered (> 10 Hz) signal difference between active and reference electrodes. Ten values were obtained during neurofeedback and ten during pauses, each calculated over five minutes of data. Statistical difference was assessed using non-parametric Wilcoxon signed ranked test given non-normally distributed values.

2.5.5. Correlation with clinical data

Pearson's correlation was computed between the mean z-normalized weighted node degree regression coefficient in the target voxels of each individual and their FMA score change (given normally distributed values).

Pearson's correlation was also tested for each voxel in the normalized space, producing a whole brain correlation map.
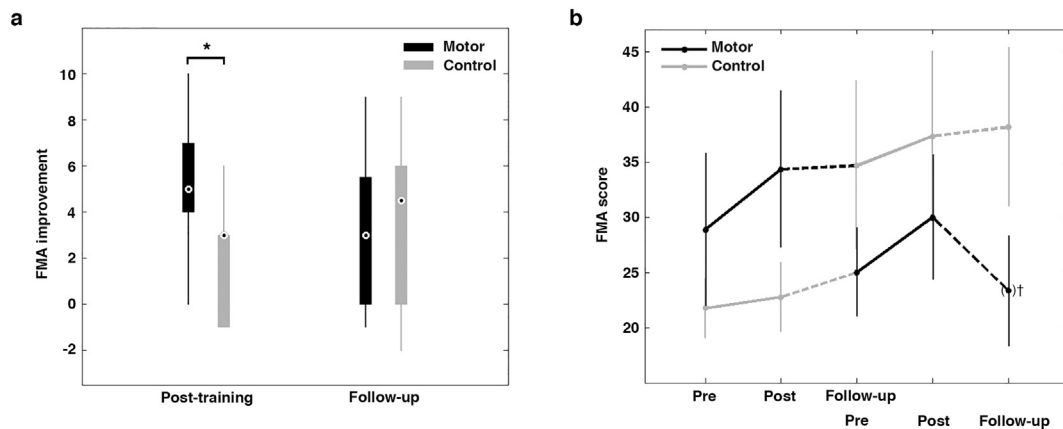
Fig. 1. Clinical effect of FC neurofeedback in the ten patients. a) Boxplot of Fugl-Meyer assessment score improvements obtained during the month of neurofeedback training, as well as at one month follow-up. * indicates a significant difference between treatment conditions (p < .05, Student's t-test). b) Mean (± standard error) evolution of the FMA score for both treatment orders. Continuous lines indicate training periods and dashed lines periods without training. † indicates one missing value.

2.5.6. Responder analysis

To explore which patients benefited the most from the intervention, we assessed the effect of patient's age, gender, stroke type, degree of internal capsule damage, initial FMA score and time since stroke on short and long-term FMA improvement. Bivariate analyses used Pearson and Spearman correlations as well as Wilcoxon rank-sum tests depending on data type and distributions. Multivariate linear regressions were then performed using significant variables of the univariate analyses.

3. Results

3.1. Clinical effects

In accordance with our main hypothesis, a significant improvement (t_9 = 5.6, p < .01) in motor performance was observed in the primary outcome measure, the FMA, between the clinical evaluation before and after the month of ipsilesional motor cortex FC training (Fig. 1a). All patients except one increased their score with a mean improvement of 5.3. During control training, there was also a significant clinical improvement (mean increase of 2.0 points, t_9 = 2.4, p = .04), but it was significantly smaller than in the active condition (t_9 = 2.4, p = .04).

Fig. 1b illustrates that improvements were seen independently of the treatment order. A mixed model ANOVA with treatment condition as within factor and treatment order as between factor confirmed a significant effect of treatment condition ($F_{1,8}$ = 5.6, p = .046) but did not show any effect of order (p = .38) and no interaction between treatment and order (p = .70).

To estimate the impact of the motor improvement elicited by our neurofeedback on different aspects such as daily living, fine dexterity or mobility, we analyzed the secondary clinical outcome measures. For all of them except grip strength, the impact was stronger during motor cortex training than control training, as presented in Table 2, but the differences were not significant. Yet, two patients were able to perform the Nine-Hole-Peg test and three the Box & Block test before treatment (the remaining patients had too severe deficits) and saw greater increase in their performance during the motor than the control training, with a mean difference of 0.24 pegs/min and 5 blocks/min in the two and three patients, respectively. The impact on daily functional tasks as measured with the Motor Activity Log–14 score was significant at p < .01 after motor cortex training, while not significant after the control training (p = .13). During motor cortex training, a meaningful mean improvement in the gait speed (> 0.06 m/s) (Perera et al., 2006) was observed, also visible in the Timed Up & Go test where two patients improved their speed above the minimal detectable threshold (> 2.9 s)

(Flansbjer et al., 2005). During the control training, the mean gait speed improvement was not meaningful (< 0.06 m/s) and one patient even decreased his speed (> 2.9 s) in the Timed Up & Go test. Levels of spasticity as measured with the Modified Ashworth Score did not significantly change during either training period (p > .38).

The significant difference between groups in the FMA score did not persist in the long term with no statistical difference between groups at one month (p = .90, Fig. 1a, but see 3.3 Responder Analysis below). In secondary outcomes, differences stayed in favor of motor cortex for most of them. A significant difference in the Time Up & Go test in favor of motor cortex training (p = .03) was observed in the long term. In the motor group, the significant impact on daily functional tasks as measured with the Motor Activity Log–14 score remained significant (p = .047) while the improvement in the European Stroke scale became significant (p = .03). Also, the mean difference in the Nine-Hole-Peg test and the Box & Block test remained in favor of motor training (difference of 1.5 pegs/min and 1.7 blocks/min respectively) and the improvement in the gait speed was meaningful only in the motor group.

3.2. Neural effects

First, we reproduced the correlation on which our neurofeedback is based for the patients of this trial. The alpha-band weighted node degree of the ipsilesional motor cortex measured during the first resting state session significantly correlated with the FMA score of the first motor evaluation (r = 0.76, p = .01).

During neurofeedback sessions, we observed a positive mean slope of the trained alpha-band weighted node degree at the targeted ipsilesional motor region (t_9 = 2.0, p = .08) (Fig. 2a and 3). The increase was significant at 10 Hz (t_9 = 2.9, p = .02) (Fig. 2b), hence suggesting that patients learned to increase the weighted node degree in the motor target area.

During control training, no change in the weighted node degree was observed in the motor target area at any alpha frequency (t < 1.0, p > .25). An increase in the contralesional prefrontal region was observed that was not significant in the entire alpha-band (p = .69) (Fig. 2c) but at 8 Hz (t_9 = 3.7, p < .01) in the targeted region (Fig. 2d).

The mean alpha-band FC change in the motor cortex of each patient correlated with the increase in FMA score during the month training (r = 0.76, p = .01) (Fig. 2f and 3), hence confirming our second hypothesis. This correlation was specific to the trained region and not seen in other brain areas on the whole-brain voxel-wise correlation map (Fig. 2e).

During the month of control training, the increase in FMA score did not correlate with the alpha-band weighted node degree slope in the

Table 2
Effect of FC neurofeedback on clinical outcome measures.

Clinical measure	Statistical test	Post-training						Follow-up					
		Motor		Control		Difference		Motor		Control		Difference	
		Mean	p-value	Mean	p-value	Mean	p-value	Mean	p-value	Mean	p-value	Mean	p-value
Fugl-Meyer (Upper Extremity) (pts/66)	t-test	5.3** ± 3.0	< 0.01	2* ± 2.6	0.04	3.3* ± 4.3	0.04	3.2* ± 3.5	0.02	3.4* ± 3.7	0.02	−0.2 ± 5.4	0.90
Box and block test (block/min)	Wilcoxon signed rank	1.4 ± 3.0	0.5	−0.1 ± 1.1	1	1.5 ± 3.6	0.5	1.1 ± 2.9	0.5	0.5 ± 1.0	0.25	0.6 ± 2.4	0.75
Nine hole peg test (peg/min)	Wilcoxon signed rank	0.43 ± 0.9	0.5	0.38 ± 1.1	0.5	0.05 ± 0.6	1	0.78 ± 1.7	0.5	0.41 ± 1.3	0.5	0.37 ± 0.66	0.5
Motor Activity Log (pts/5)	Wilcoxon signed rank	0.3** ± 0.2	< 0.01	0.2 ± 0.3	0.13	0.1 ± 0.3	0.49	0.3* ± 0.4	0.05	0.4† ± 0.5	0.07	−0.1 ± 0.4	0.64
10 m Walk (m/s)	Wilcoxon signed rank	0.10 ± 0.2	0.11	0.04 ± 0.1	0.20	0.06 ± 0.2	0.55	0.09† ± 0.1	0.06	0.01 ± 0.1	0.73	0.08 ± 0.2	0.31
Timed up and go (s)	Wilcoxon signed rank	−2.0 ± 4.4	0.95	1.0 ± 3.6	1	−3.0 ± 7.7	0.82	−3.4* ± 3.4	0.03	−0.2 ± 5.1	0.43	−3.2* ± 5.0	0.03
European Stroke Scale (pts/100)	Wilcoxon signed rank	1.4 ± 2.2	0.13	0.4 ± 0.7	0.25	1 ± 2.2	0.25	2.8* ± 2.3	0.03	1.7† ± 2.0	0.06	1.0 ± 3.5	0.44
MRC muscle strength scale (pts/35)	Wilcoxon signed rank	0.9 ± 2.5	0.50	−0.1 ± 0.3	1	1.0 ± 2.5	0.50	0.8 ± 2.0	0.5	0.1 ± 0.7	1	0.7 ± 2.2	0.75
Jamar (kg)	Wilcoxon signed rank	−0.4 ± 1.3	0.37	0.3 ± 2.7	0.72	−0.8 ± 2.4	0.39	0.2 ± 3.4	0.84	1.6 ± 3.8	0.22	−1.6 ± 7.1	0.69
Modified Ashworth scale (pts/35)	Wilcoxon signed rank	−0.3 ± 0.8	0.38	0.1 ± 1.5	1	−0.3 ± 2.0	0.88	−0.3 ± 0.8	0.50	−0.6 ± 0.9	0.13	0.3 ± 1.2	0.38

Value are mean ± SD
** Significant at $p < .01$.
* Significant at $p < .05$.
† Marginally significant at $p < .1$.

control target area ($r = -0.40$, $p = .26$) or with the alpha-band FC change between the control area and the ipsilesional motor area ($r = -0.15$, p = .69).

Given the FC enhancement of the motor target area as indicated by an increased weighted node degree, we explored which interactions were most concerned by this enhancement. We found significantly increased FC with ipsilateral fronto-temporal areas. However, in contrast to the weighted node degree, the specific FC increases between the motor target area and fronto-temporal areas did not correlate with motor improvement ($r = 0.06$, $p = .86$).

The alpha-band weighted node degree at the motor target region also increased during the eight pre-session resting-state recordings over the month of motor neurofeedback training, but only in patients showing an FMA improvement > 5 ($N = 4$, p = .02).

To verify that the effect of the neurofeedback was not due to a modulation of power in the target region, we measured the change in alpha-band power at the targeted motor region during active neurofeedback periods and found it not to be significant ($p = .65$). Power changes did not significantly correlate with the slope of alpha-band weighted node degree ($r = -0.20$, $p = .58$) or with the improvement in the FMA score ($r = -0.46$, $p = .18$).

3.3. Responder analysis

With regards to long-term improvement, univariate analyses found an effect of lesion side (W = 28.5, $p = .048$) and time since stroke ($r = 0.70$, p = .04), but for none of the other variables ($r < 0.32$, $p > .40$; W < 24, $p > .33$). In a multivariate analysis, only lesion side (beta = −3.92, $t = -2.28$, $p = .06$) remained marginally significant but not time ($t = 1.41$, $p = .21$). The negative impact of right lesions on retention is shown in Fig. 4.

No predictor was significant in a multivariate model of short-term improvement ($p > .26$).

3.4. Movement confounders

None of the patients reported the use a motor imagery strategy for the neurofeedback task. The electromyography of the abductor pollicis and extensor carpi radialis confirmed that patients did not contract their upper limb muscles during neurofeedback. The first patient presented a mean muscle contraction estimated with root mean square amplitude of 4.1 µV during neurofeedback and 4.7 µV during pauses ($p = .38$) and the second patient a mean contraction of 8.9 µV during neurofeedback and 9.4 µV during pauses ($p = .19$).

4. Discussion

An increasing number of empirical and theoretical studies investigate brain function through a network perspective. We demonstrated here by a direct and voluntary manipulation of FC through neurofeedback that a targeted change in FC at a specific brain area and frequency band has a proportional impact on behaviour, bringing evidence on the causal influence of FC on brain function. Such demonstrations are crucial to help elucidate the neural substrate of brain disease and for providing a rationale for the usage of FC in the search for biomarkers and treatment targets.

We already know that FC cannot be reduced to a mere reflection of structural connectivity. While strong functional interactions exist between areas with strong structural connections (Hermundstad et al., 2013; Tewarie et al., 2014; van den Heuvel et al., 2009), structural connectivity cannot entirely predict FC (Honey et al., 2009). FC may arise via indirect anatomical connections, which partially explains missing correspondence. Dynamics of brain activity during resting-state explain another part (Deco et al., 2011). FC exhibits indeed variability across recording sessions but also within runs at faster time-scales (Hutchison et al., 2013; Sadaghiani et al., 2015). This ongoing variation
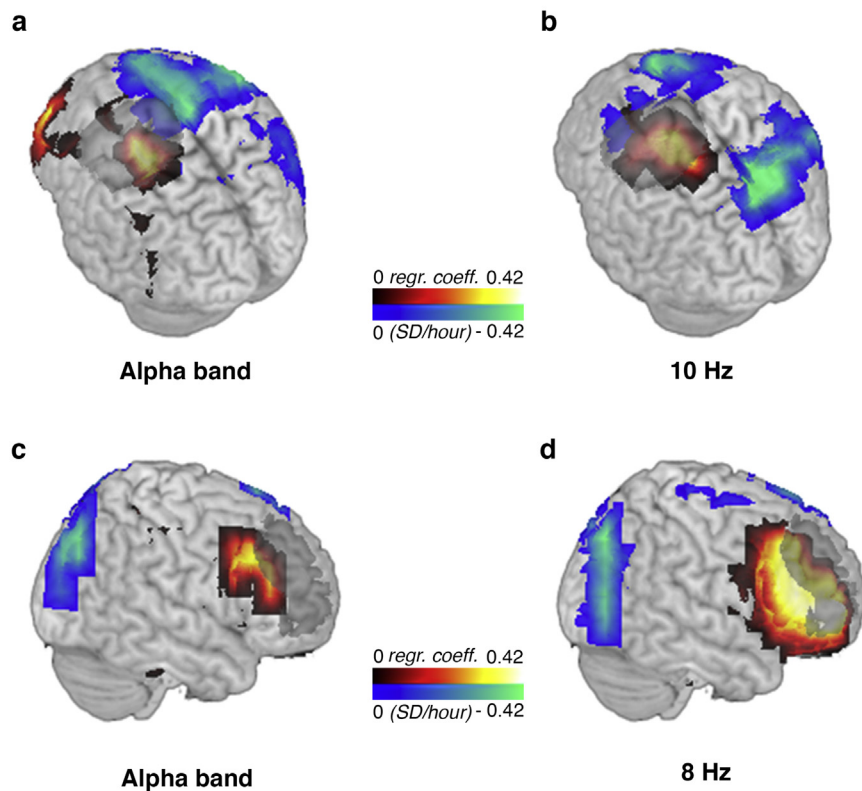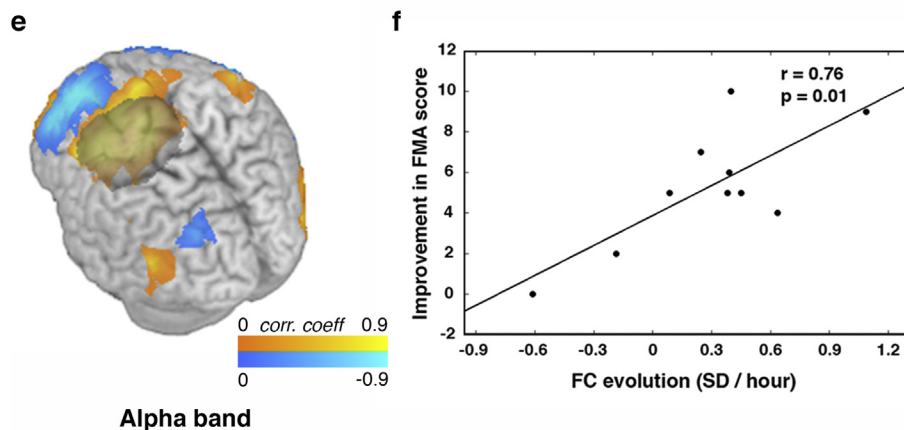
FC (node degree) evolution during neurofeedback

a

Alpha band

b

10 Hz

0 *regr. coeff.* 0.42
0 *(SD/hour)* - 0.42

c

Alpha band

d

8 Hz

0 *regr. coeff.* 0.42
0 *(SD/hour)* - 0.42

Correlation FC (node degree) evolution - motor performance

e

Alpha band

0 *corr. coeff* 0.9
0 -0.9

f

r = 0.76
p = 0.01

Improvement in FMA score

FC evolution (SD / hour)

Fig. 2. Neural effect of the FC neurofeedback in the ten patients. Regions showing a significant modulation (red and blue colors) of the weighted node degree in the alpha-band (a) and at 10 Hz (b) during the neurofeedback sessions targeting the ipsilesional motor cortex (marked in grey). Regions showing a significant modulation (red and blue colors) of the weighted node degree in the alpha-band (c) and at 8 Hz (d) during the neurofeedback sessions targeting the contralesional prefrontal cortex (marked in grey). e) Regions showing a correlation between enhancements in alpha-band weighted node degree at the ipsilesional motor cortex (grey area) and change in the upper extremity FMA score. f) Enhancements of alpha-band weighted node degree at the targeted ipsilesional motor cortex were associated with a proportional increase in the upper extremity FMA score.

of activity has been proposed to represent fluctuations between segregation and integration states at many spatio-temporal scales (Sporns, 2013). It is thought to reflect an internal model shaped by previous experience and individual connectivity biases that impact behavior by providing a necessary operational context (Harmelech and Malach, 2013; Raichle and Snyder, 2007). A further mechanisms by which FC impacts behavior may be related to processing of previous experience and consolidation of learning (Miall and Robertson, 2006). FC is indeed modulated proportionally to learning immediately after a motor or sensory task (Albert et al., 2009; Lewis et al., 2009). The FC pattern we chose to train was based on an observed correlation with behavior (Dubovik et al., 2012; Guggisberg et al., 2015). It can be interpreted as

an integration of a given cortical region into large-scale brain networks. The alpha-band is indeed implicated in long range synchronization (Doesburg et al., 2009; Hummel and Gerloff, 2005; Palva and Palva, 2007). This may have contributed to an enlargement of the motor network with recruitment of additional areas.

FC enhancements of the motor target concerned preferentially interactions with fronto-temporal areas of the same hemisphere. However, the correlation analyses suggest that not specific interactions with these areas, but an FC enhancement across the network were associated with better motor recovery. Hence, FC increases do not need to concern interactions with specific brain regions, as long as the overall interaction of the target area with the entire brain are enhanced. This
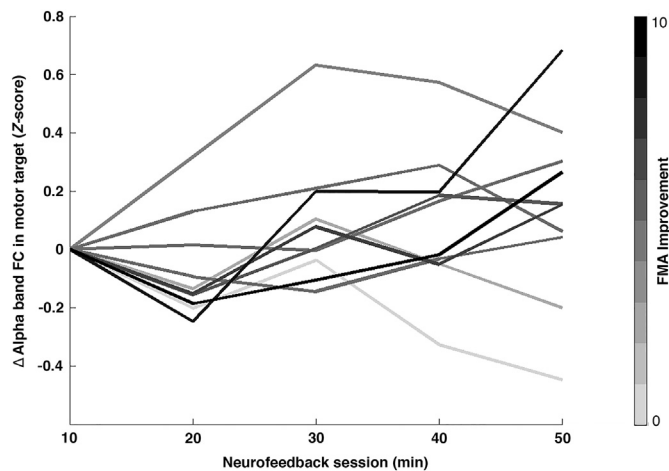
Fig. 3. FC evolution during neurofeedback sessions. Each line represents the evolution in one patient of its FC during neurofeedback sessions, averaged over the eight sessions. FC values are the alpha-band weighted node degree calculated over ten minutes of neurofeedback (z-normalized). The color scale indicates the individual motor improvement as measured with the FMA score.
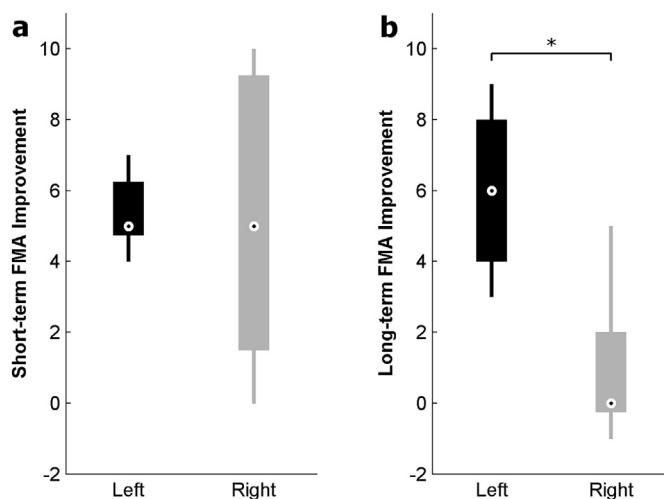
Fig. 4. FMA score improvement in patients with a right-sided (grey) and a left-sided (black) lesion after the neurofeedback sessions targeting the ipsilesional motor cortex (a) and at one-month follow-up (b). * Indicates a significant difference in long-term FMA improvement between patients with left-sided and right-sided lesions (p < .05, Wilcoxon rank-sum test).

may be a particularity of alpha-band interactions. A previous study observed that alpha-band networks differ from resting-state networks as observed in functional resonance imaging. The former are implicated in global integration across networks and the latter in communication within specific networks and between hemispheres (Guggisberg et al., 2015).

Long distance cortical coupling in the alpha-band has been related to modulation of sensori-motor beta-band power (Vukelic et al., 2014; Vukelic and Gharabaghi, 2015a, 2015b). Beta-band is known to mediate effective, frequency- and phase-specific cortico-spinal communication (Khademi et al., 2018) while neurofeedback of beta-band power increases corticospinal connectivity (Belardinelli et al., 2017; Kraus et al., 2016b) and motor behavior (Naros and Gharabaghi, 2015). Our neurofeedback effect on alpha-band connectivity could have been translated to actual motor improvement through cross-frequency interactions improving beta-band modulation hereby increasing, ultimately, cortico-spinal communication.

Despite the specific efficacy of FC training in the short term, it did

not lead to a long-term retention of the clinical improvement in all patients. Although this is also the case for many other rehabilitation treatments, it limits applications in practice. Long-term improvement requires that patients reach a threshold of improvement which then enables the integration of motor improvements into activities of daily living (Han et al., 2008; Kleim and Jones, 2008). Enhancing the effect of our neurofeedback training may thus lead to better long-term retention. Increasing training intensity could be one strategy since dose of motor rehabilitation intervention in chronic stroke patients enhances gains in motor function (Byl et al., 2008; Hsieh et al., 2012). Adding other modalities such as peripheral or brain stimulation (Kraus et al., 2016a; Kraus et al., 2018) or pharmacological intervention such as fluoxetine (Chollet et al., 2011; Mead et al., 2013) to induce plasticity may also potentiate the approach. A key factor for retention in our study was the side of the lesion. Patients with a lesion in the right hemisphere demonstrated variable short-term improvement and significantly lower long-term improvement compared to patients with a left-sided lesion (Fig. 4). There is some evidence that right lesions, in particular right parietal lesions are associated with worse outcome and less recovery (Aszalos et al., 2002; Bentley et al., 2014; Rangaraju et al., 2015; Yassi et al., 2015). Furthermore, right lesions often lead to visuospatial neglect that is known to have a negative impact on rehabilitation (Gerafi et al., 2017). None of our patients had severe neglect, but mild residual neglect might have contributed to low retention. Applying network neurofeedback therapy to patients with left hemispheric lesions seems to lead to better long-term effects.

Our physical therapy sessions preceded the neurofeedback trainings with the idea that FC training would help consolidate motor learning. However, FC could also provide an optimal operational context for motor learning, in which case it may have been more beneficial to schedule physical therapy after neurofeedback. A more thorough understanding of the dynamics of FC and more particularly alpha-band node degree in relation to motor learning could help decide how to best combine motor exercises and FC training in the future. This along with a better understanding of which patients benefit the most from the therapy may then also lead to better retention.

Several technical difficulties to the intervention provided here need to be considered. First, our study intended to directly target FC in order to provide evidence that such strategies can be causally effective for reducing neurological deficits. However, modulating FC of brain areas is technically challenging and requires high-density EEG with long setup times. Other approaches may enable an *indirect* enhancement of FC while being easier to implement in clinical practice. For instance, neurofeedback of circumscribed motor activations can modulate FC (Vukelic and Gharabaghi, 2015a) but requires only few EEG electrodes and enables shorter feedback delays. Non-invasive brain stimulation induces changes in FC during and after stimulation (Krawinkel et al., 2015; Meinzer et al., 2012; Pena-Gomez et al., 2012; Polania et al., 2012; Rizk et al., 2013; Sale et al., 2015; Sehm et al., 2012; Volz et al., 2016). Behavioral interventions also modify FC (Freyer et al., 2012; Solca et al., 2016). Nevertheless, our approach enables a more selective and specific modulation of FC, which may be important for certain applications.

Second, the usage of resting-state data to compute the spatial filter may have led to suboptimal real-time source activity calculation, the optimization being based on data having potentially other sources of noise. We tested this in three patients of the present trial by using the immediately preceding neurofeedback block rather than the resting-state recording to compute the spatial filter. The FMA gain (p = .69) and the difference in FMA gain between conditions (p = .76) were not greater in these three patients, hence suggesting that this was not a major problem.

Third, IC was used as index of FC because of its computational simplicity, which was of particular advantage in a real-time setting. However, IC has the disadvantage that its magnitude depends not only on the strength of coupling, but also on the phase lag. Neurofeedback

training could hence have induced a systematic change in phase lags between brain regions towards a lag of π/2 or -π/2. However, we did not observe a significant decrease in the real component of coherency (representing zero-lag coupling, *p* = .34). Moreover, if the induced changes had concerned exclusively a shift in lag, we should have observed a negative correlation between changes in real and imaginary coherence. This was not the case in our data (*r* = 0.14, *p* = .71). Yet, future implementations of network neurofeedback could choose other indices of FC to avoid this possibility.

Fourth, the real-time computation of FC introduces a feedback delay, which could hinder learning. On the other hand, neurofeedback with functional magnetic resonance imaging implicates even longer physiological lags and has been proven feasible (Koush et al., 2017).

Finally, refined neurofeedback approaches include also adjusting the difficulty level in a more systematic way, e.g. by taking into account for the cognitive load and the learning experience of patients (Naros and Gharabaghi, 2015; Naros et al., 2016).

Interestingly, we also observed an increase in weighted node degree at the contralesional prefrontal control region, but it concerned mainly frequencies around 8 Hz and not the whole alpha-band, while significant increase in motor target area was more around 10 Hz. This may be due to the well-known predominance of alpha rhythms at motor and posterior brain areas, while prefrontal regions operate preferentially through long-range synchronization in the theta band (Sarnthein et al., 1998; Sauseng et al., 2010; von Stein and Sarnthein, 2000). Neurofeedback training may have led to an enhancement of low alpha frequencies because they are closer to the intrinsic rhythms of this area.

Funding

Conflict of interest

The authors declare no competing financial interests.

References

Albert, N.B., Robertson, E.M., Miall, R.C., 2009. The resting human brain and motor learning. Curr. Biol. 19, 1023–1027.

Aszalos, Z., Barsi, P., Vitrai, J., Nagy, Z., 2002. Lateralization as a factor in the prognosis of middle cerebral artery territorial infarct. Eur. Neurol. 48, 141–145.

Baldassarre, A., Ramsey, L., Rengachary, J., Zinn, K., Siegel, J.S., Metcalf, N.V., Strube, M.J., Snyder, A.Z., Corbetta, M., Shulman, G.L., 2016. Dissociated functional connectivity profiles for motor and attention deficits in acute right-hemisphere stroke. Brain 139, 2024–2038.

Bassett, D.S., Khambhati, A.N., 2017. A network engineering perspective on probing and perturbing cognition with neurofeedback. Ann. N. Y. Acad. Sci. 1396, 126–143.

Belardinelli, P., Laer, L., Ortiz, E., Braun, C., Gharabaghi, A., 2017. Plasticity of premotor cortico-muscular coherence in severely impaired stroke patients with hand paralysis. Neuroimage Clin. 14, 726–733.

Bentley, P., Kumar, G., Rinne, P., Buddha, S., Kallingal, J., Hookway, C., Sharma, P., Mehta, A., Beckmann, C., 2014. Lesion locations influencing baseline severity and early recovery in ischaemic stroke. Eur. J. Neurol. 21, 1226–1232.

Bohannon, R.W., Smith, M.B., 1987. Interrater reliability of a modified Ashworth scale of muscle spasticity. Phys. Ther. 67, 206–207.

Brett, M., Leff, A.P., Rorden, C., Ashburner, J., 2001. Spatial normalization of brain images with focal lesions using cost function masking. NeuroImage 14, 486–500.

Byl, N.N., Pitsch, E.A., Abrams, G.M., 2008. Functional outcomes can vary by dose: learning-based sensorimotor training for patients stable poststroke. Neurorehabil. Neural Repair 22, 494–504.

Carter, A.R., Astafiev, S.V., Lang, C.E., Connor, L.T., Rengachary, J., Strube, M.J., Pope, D.L., Shulman, G.L., Corbetta, M., 2010. Resting interhemispheric functional magnetic resonance imaging connectivity predicts performance after stroke. Ann. Neurol. 67, 365–375.

Chollet, F., Tardy, J., Albucher, J.F., Thalamas, C., Berard, E., Lamy, C., Bejot, Y., Deltour, S., Jaillard, A., Niclot, P., Guillon, B., Moulin, T., Marque, P., Pariente, J., Arnaud, C., Loubinoux, I., 2011. Fluoxetine for motor recovery after acute ischaemic stroke (FLAME): a randomised placebo-controlled trial. Lancet Neurol. 10, 123–130.

Compston, A., 2010. Aids to the investigation of peripheral nerve injuries. Medical Research Council: Nerve Injuries Research Committee. His Majesty's Stationery Office: 1942; pp. 48 (iii) and 74 figures and 7 diagrams; with aids to the examination of the peripheral nervous system. 133. By Michael O'Brien for the Guarantors of

Brain. Saunders Elsevier, pp. 2838–2844 (pp. [8] 64 and 94 Figures. Brain).

Dalal, S.S., Zumer, J.M., Guggisberg, A.G., Trumpis, M., Wong, D.D., Sekihara, K., Nagarajan, S.S., 2011. MEG/EEG source reconstruction, statistical evaluation, and visualization with NUTMEG. Comput. Intell. Neurosci. 2011, 758973.

Damoiseaux, J.S., Rombouts, S.A., Barkhof, F., Scheltens, P., Stam, C.J., Smith, S.M., Beckmann, C.F., 2006. Consistent resting-state networks across healthy subjects. Proc. Natl. Acad. Sci. U. S. A. 103, 13848–13853.

Davis, S.W., Stanley, M.L., Moscovitch, M., Cabeza, R., 2017. Resting-state networks do not determine cognitive function networks: a commentary on Campbell and Schacter (2016). Lang Cogn Neurosci 32, 669–673.

Deco, G., Jirsa, V.K., McIntosh, A.R., 2011. Emerging concepts for the dynamical organization of resting-state activity in the brain. Nat. Rev. Neurosci. 12, 43–56.

Deriche, R., 2016. Computational brain connectivity mapping: a core health and scientific challenge. Med. Image Anal. 33, 122–126.

Doesburg, S.M., Green, J.J., McDonald, J.J., Ward, L.M., 2009. From local inhibition to long-range integration: a functional dissociation of alpha-band synchronization across cortical scales in visuospatial attention. Brain Res. 1303, 97–110.

Dubovik, S., Pignat, J.M., Ptak, R., Aboulafia, T., Allet, L., Gillabert, N., Magnin, C., Albert, F., Momjian-Mayor, I., Nahum, L., Lascano, A.M., Michel, C.M., Schnider, A., Guggisberg, A.G., 2012. The behavioral significance of coherent resting-state oscillations after stroke. NeuroImage 61, 249–257.

Fellrath, J., Mottaz, A., Schnider, A., Guggisberg, A.G., Ptak, R., 2016. Theta-band functional connectivity in the dorsal fronto-parietal network predicts goal-directed attention. Neuropsychologia 92, 20–30.

Flansbjer, U.B., Holmback, A.M., Downham, D., Patten, C., Lexell, J., 2005. Reliability of gait performance tests in men and women with hemiparesis after stroke. J. Rehabil. Med. 37, 75–82.

Fox, M.D., Greicius, M., 2010. Clinical applications of resting state functional connectivity. Front. Syst. Neurosci. 4, 19.

Freyer, F., Reinacher, M., Nolte, G., Dinse, H.R., Ritter, P., 2012. Repetitive tactile stimulation changes resting-state functional connectivity-implications for treatment of sensorimotor decline. Front. Hum. Neurosci. 6, 144.

Fries, P., 2005. A mechanism for cognitive dynamics: neuronal communication through neuronal coherence. Trends Cogn. Sci. 9, 474–480.

Fugl-Meyer, A.R., Jaasko, L., Leyman, I., Olsson, S., Steglind, S., 1975. The post-stroke hemiplegic patient. 1. A method for evaluation of physical performance. Scand. J. Rehabil. Med. 7, 13–31.

Gerafi, J., Samuelsson, H., Viken, J.I., Blomgren, C., Claesson, L., Kallio, S., Jern, C., Blomstrand, C., Jood, K., 2017. Neglect and aphasia in the acute phase as predictors of functional outcome 7 years after ischemic stroke. Eur. J. Neurol. 24, 1407–1415.

Gladstone, D.J., Danells, C.J., Black, S.E., 2002. The fugl-meyer assessment of motor recovery after stroke: a critical review of its measurement properties. Neurorehabil. Neural Repair 16, 232–240.

Greicius, M.D., Krasnow, B., Reiss, A.L., Menon, V., 2003. Functional connectivity in the resting brain: a network analysis of the default mode hypothesis. Proc. Natl. Acad. Sci. U. S. A. 100, 253–258.

Guggisberg, A.G., Rizk, S., Ptak, R., Di Pietro, M., Saj, A., Lazeyras, F., Lovblad, K.O., Schnider, A., Pignat, J.M., 2015. Two intrinsic coupling types for resting-state integration in the human brain. Brain Topogr. 28, 318–329.

Hampson, M., Driesen, N.R., Skudlarski, P., Gore, J.C., Constable, R.T., 2006. Brain connectivity related to working memory performance. J. Neurosci. 26, 13338–13343.

Han, C.E., Arbib, M.A., Schweighofer, N., 2008. Stroke rehabilitation reaches a threshold. PLoS Comput. Biol. 4, e1000133.

Hantson, L., De Weerdt, W., De Keyser, J., Diener, H.C., Franke, C., Palm, R., Van Orshoven, M., Schoonderwalt, H., De Klippel, N., Herroelen, L., 1994. The European stroke scale. Stroke 25, 2215–2219.

Harmelech, T., Malach, R., 2013. Neurocognitive biases and the patterns of spontaneous correlations in the human cortex. Trends Cogn. Sci. 17, 606–615.

He, B.J., Snyder, A.Z., Vincent, J.L., Epstein, A., Shulman, G.L., Corbetta, M., 2007. Breakdown of functional connectivity in frontoparietal networks underlies behavioral deficits in spatial neglect. Neuron 53, 905–918.

Hermundstad, A.M., Bassett, D.S., Brown, K.S., Aminoff, E.M., Clewett, D., Freeman, S., Frithsen, A., Johnson, A., Tipper, C.M., Miller, M.B., Grafton, S.T., Carlson, J.M., 2013. Structural foundations of resting-state and task-based functional connectivity in the human brain. Proc. Natl. Acad. Sci. U. S. A. 110, 6169–6174.

Hipp, J.F., Engel, A.K., Siegel, M., 2011. Oscillatory synchronization in large-scale cortical networks predicts perception. Neuron 69, 387–396.

Honey, C.J., Sporns, O., Cammoun, L., Gigandet, X., Thiran, J.P., Meuli, R., Hagmann, P., 2009. Predicting human resting-state functional connectivity from structural connectivity. Proc. Natl. Acad. Sci. U. S. A. 106, 2035–2040.

Hsieh, Y.W., Wu, C.Y., Lin, K.C., Yao, G., Wu, K.Y., Chang, Y.J., 2012. Dose-response relationship of robot-assisted stroke motor rehabilitation: the impact of initial motor status. Stroke 43, 2729–2734.

Hummel, F., Gerloff, C., 2005. Larger interregional synchrony is associated with greater behavioral success in a complex sensory integration task in humans. Cereb. Cortex 15, 670–678.

Hutchison, R.M., Womelsdorf, T., Allen, E.A., Bandettini, P.A., Calhoun, V.D., Corbetta, M., Della Penna, S., Duyn, J.H., Glover, G.H., Gonzalez-Castillo, J., Handwerker, D.A., Keilholz, S., Kiviniemi, V., Leopold, D.A., de Pasquale, F., Sporns, O., Walter, M., Chang, C., 2013. Dynamic functional connectivity: promise, issues, and interpretations. NeuroImage 80, 360–378.

Kajal, D.S., Braun, C., Mellinger, J., Sacchet, M.D., Ruiz, S., Fetz, E., Birbaumer, N., Sitaram, R., 2017. Learned control of inter-hemispheric connectivity: effects on bimanual motor performance. Hum. Brain Mapp. 38, 4353–4369.

Kellor, M., Frost, J., Silberberg, N., Iversen, I., Cummings, R., 1971. Hand strength and dexterity. Am. J. Occup. Ther. 25, 77–83.

Khademi, F., Royter, V., Gharabaghi, A., 2018. Distinct Beta-band oscillatory circuits underlie corticospinal gain modulation. Cereb. Cortex 28, 1502–1515.

Kleim, J.A., Jones, T.A., 2008. Principles of experience-dependent neural plasticity: implications for rehabilitation after brain damage. J Speech Lang Hear Res 51, S225–S239.

Koush, Y., Meskaldji, D.E., Pichon, S., Rey, G., Rieger, S.W., Linden, D.E., Van De Ville, D., Vuilleumier, P., Scharnowski, F., 2017. Learning control over emotion networks through connectivity-based neurofeedback. Cereb. Cortex 27, 1193–1202.

Kraus, D., Naros, G., Bauer, R., Khademi, F., Leao, M.T., Ziemann, U., Gharabaghi, A., 2016a. Brain state-dependent transcranial magnetic closed-loop stimulation controlled by sensorimotor desynchronization induces robust increase of corticospinal excitability. Brain Stimul 9, 415–424.

Kraus, D., Naros, G., Bauer, R., Leao, M.T., Ziemann, U., Gharabaghi, A., 2016b. Brain-robot interface driven plasticity: distributed modulation of corticospinal excitability. NeuroImage 125, 522–532.

Kraus, D., Naros, G., Guggenberger, R., Leao, M.T., Ziemann, U., Gharabaghi, A., 2018. Recruitment of additional corticospinal pathways in the human brain with state-dependent paired associative stimulation. J. Neurosci. 38, 1396–1407.

Krawinkel, L.A., Engel, A.K., Hummel, F.C., 2015. Modulating pathological oscillations by rhythmic non-invasive brain stimulation-a therapeutic concept? Front. Syst. Neurosci. 9, 33.

Lewis, C.M., Baldassarre, A., Committeri, G., Romani, G.L., Corbetta, M., 2009. Learning sculpts the spontaneous activity of the resting human brain. Proc. Natl. Acad. Sci. U. S. A. 106, 17558–17563.

Liew, S.L., Rana, M., Cornelsen, S., Fortunato de Barros Filho, M., Birbaumer, N., Sitaram, R., Cohen, L.G., Soekadar, S.R., 2016. Improving motor Corticothalamic communication after stroke using real-time fMRI connectivity-based neurofeedback. Neurorehabil. Neural Repair 30, 671–675.

Lin, K.C., Chuang, L.L., Wu, C.Y., Hsieh, Y.W., Chang, W.Y., 2010. Responsiveness and validity of three dexterous function measures in stroke rehabilitation. J. Rehabil. Res. Dev. 47, 563–571.

Mathiowetz, V., Volland, G., Kashman, N., Weber, K., 1985. Adult norms for the box and block test of manual dexterity. Am. J. Occup. Ther. 39, 386–391.

Mead, G.E., Hsieh, C.F., Lee, R., Kutlubaev, M., Claxton, A., Hankey, G.J., Hackett, M., 2013. Selective serotonin reuptake inhibitors for stroke recovery: a systematic review and meta-analysis. Stroke 44, 844–850.

Meinzer, M., Antonenko, D., Lindenberg, R., Hetzer, S., Ulm, L., Avirame, K., Flaisch, T., Floel, A., 2012. Electrical brain stimulation improves cognitive performance by modulating functional connectivity and task-specific activation. J. Neurosci. 32, 1859–1866.

Miall, R.C., Robertson, E.M., 2006. Functional imaging: is the resting brain resting? Curr. Biol. 16, R998–1000.

Mottaz, A., Solca, M., Magnin, C., Corbet, T., Schnider, A., Guggisberg, A.G., 2015. Neurofeedback training of alpha-band coherence enhances motor performance. Clin. Neurophysiol. 126, 1754–1760.

Naros, G., Gharabaghi, A., 2015. Reinforcement learning of self-regulated beta-oscillations for motor restoration in chronic stroke. Front. Hum. Neurosci. 9, 391.

Naros, G., Naros, I., Grimm, F., Ziemann, U., Gharabaghi, A., 2016. Reinforcement learning of self-regulated sensorimotor beta-oscillations improves motor performance. NeuroImage 134, 142–152.

Newman, M.E., 2004. Analysis of weighted networks. Phys. Rev. E Stat. Nonlinear Soft Matter Phys. 70, 056131.

Nicolo, P., Rizk, S., Magnin, C., Pietro, M.D., Schnider, A., Guggisberg, A.G., 2015. Coherent neural oscillations predict future motor and language improvement after stroke. Brain 138, 3048–3060.

Nolte, G., Bai, O., Wheaton, L., Mari, Z., Vorbach, S., Hallett, M., 2004. Identifying true brain interaction from EEG data using the imaginary part of coherency. Clin. Neurophysiol. 115, 2292–2307.

Oostenveld, R., Fries, P., Maris, E., Schoffelen, J.M., 2011. FieldTrip: open source software for advanced analysis of MEG, EEG, and invasive electrophysiological data. Comput Intell Neurosci 2011, 156869.

Palva, S., Palva, J.M., 2007. New vistas for alpha-frequency band oscillations. Trends Neurosci. 30, 150–158.

Pena-Gomez, C., Sala-Lonch, R., Junque, C., Clemente, I.C., Vidal, D., Bargallo, N., Falcon, C., Valls-Sole, J., Pascual-Leone, A., Bartres-Faz, D., 2012. Modulation of large-scale brain networks by transcranial direct current stimulation evidenced by resting-state functional MRI. Brain Stimul 5, 252–263.

Perera, S., Mody, S.H., Woodman, R.C., Studenski, S.A., 2006. Meaningful change and responsiveness in common physical performance measures in older adults. J. Am. Geriatr. Soc. 54, 743–749.

Polania, R., Paulus, W., Nitsche, M.A., 2012. Reorganizing the intrinsic functional architecture of the human primary motor cortex during rest with non-invasive cortical stimulation. PLoS One 7, e30971.

Poldrack, R.A., Farah, M.J., 2015. Progress and challenges in probing the human brain. Nature 526, 371–379.

Raichle, M.E., Snyder, A.Z., 2007. A default mode of brain function: a brief history of an evolving idea. NeuroImage 37, 1083–1090 (discussion 1097-1089).

Ramnani, N., Owen, A.M., 2004. Anterior prefrontal cortex: insights into function from anatomy and neuroimaging. Nat. Rev. Neurosci. 5, 184–194.

Ramot, M., Kimmich, S., Gonzalez-Castillo, J., Roopchansingh, V., Popal, H., White, E., Gotts, S.J., Martin, A., 2017. Direct modulation of aberrant brain network connectivity through real-time NeuroFeedback. elife 6.

Rangaraju, S., Streib, C., Aghaebrahim, A., Jadhav, A., Frankel, M., Jovin, T.G., 2015. Relationship between lesion topology and clinical outcome in anterior circulation large vessel occlusions. Stroke 46, 1787–1792.

Rehme, A.K., Eickhoff, S.B., Grefkes, C., 2013. State-dependent differences between functional and effective connectivity of the human cortical motor system. NeuroImage 67, 237–246.

Rizk, S., Ptak, R., Nyffeler, T., Schnider, A., Guggisberg, A.G., 2013. Network mechanisms of responsiveness to continuous theta-burst stimulation. Eur. J. Neurosci. 38, 3230–3238.

Sacchet, M.D., Mellinger, J., Sitaram, R., Braun, C., Birbaumer, N., Fetz, E., 2012. Volitional control of neuromagnetic coherence. Front. Neurosci. 6, 189.

Sadaghiani, S., Poline, J.B., Kleinschmidt, A., D'Esposito, M., 2015. Ongoing dynamics in large-scale functional connectivity predict perception. Proc. Natl. Acad. Sci. U. S. A. 112, 8463–8468.

Sale, M.V., Mattingley, J.B., Zalesky, A., Cocchi, L., 2015. Imaging human brain networks to improve the clinical efficacy of non-invasive brain stimulation. Neurosci. Biobehav. Rev. 57, 187–198.

Sami, S., Robertson, E.M., Miall, R.C., 2014. The time course of task-specific memory consolidation effects in resting state networks. J. Neurosci. 34, 3982–3992.

Sarnthein, J., Petsche, H., Rappelsberger, P., Shaw, G.L., von Stein, A., 1998. Synchronization between prefrontal and posterior association cortex during human working memory. Proc. Natl. Acad. Sci. U. S. A. 95, 7092–7096.

Sauseng, P., Griesmayr, B., Freunberger, R., Klimesch, W., 2010. Control mechanisms in working memory: a possible function of EEG theta oscillations. Neurosci. Biobehav. Rev. 34, 1015–1022.

Schlee, W., Leirer, V., Kolassa, I.T., Weisz, N., Elbert, T., 2012. Age-related changes in neural functional connectivity and its behavioral relevance. BMC Neurosci. 13, 16.

Schmidt, R.T., Toews, J.V., 1970. Grip strength as measured by the Jamar dynamometer. Arch. Phys. Med. Rehabil. 51, 321–327.

Sehm, B., Schafer, A., Kipping, J., Margulies, D., Conde, V., Taubert, M., Villringer, A., Ragert, P., 2012. Dynamic modulation of intrinsic functional connectivity by transcranial direct current stimulation. J. Neurophysiol. 108, 3253–3263.

Sekihara, K., Nagarajan, S.S., Poeppel, D., Marantz, A., 2004. Asymptotic SNR of scalar and vector minimum-variance beamformers for neuromagnetic source reconstruction. IEEE Trans. Biomed. Eng. 51, 1726–1734.

Sekihara, K., Owen, J.P., Trisno, S., Nagarajan, S.S., 2011. Removal of spurious coherence in MEG source-space coherence analysis. IEEE Trans. Biomed. Eng. 58, 3121–3129.

Sharma, N., Baron, J.C., Rowe, J.B., 2009. Motor imagery after stroke: relating outcome to motor network connectivity. Ann. Neurol. 66, 604–616.

Singh, K.D., Barnes, G.R., Hillebrand, A., 2003. Group imaging of task-related changes in cortical synchronisation using nonparametric permutation testing. NeuroImage 19, 1589–1601.

Solca, M., Mottaz, A., Guggisberg, A.G., 2016. Binaural beats increase interhemispheric alpha-band coherence between auditory cortices. Hear. Res. 332, 233–237.

Sporns, O., 2013. Network attributes for segregation and integration in the human brain. Curr. Opin. Neurobiol. 23, 162–171.

Stam, C.J., van Straaten, E.C., 2012. The organization of physiological brain networks. Clin. Neurophysiol. 123, 1067–1087.

Stenroos, M., Mantynen, V., Nenonen, J., 2007. A Matlab library for solving quasi-static volume conduction problems using the boundary element method. Comput. Methods Prog. Biomed. 88, 256–263.

Sun, F.T., Miller, L.M., Rao, A.A., D'Esposito, M., 2007. Functional connectivity of cortical networks involved in bimanual motor sequence learning. Cereb. Cortex 17, 1227–1234.

Tambini, A., Ketz, N., Davachi, L., 2010. Enhanced brain correlations during rest are related to memory for recent experiences. Neuron 65, 280–290.

Tewarie, P., Hillebrand, A., van Dellen, E., Schoonheim, M.M., Barkhof, F., Polman, C.H., Beaulieu, C., Gong, G., van Dijk, B.W., Stam, C.J., 2014. Structural degree predicts functional network connectivity: a multimodal resting-state fMRI and MEG study. NeuroImage 97, 296–307.

Uswatte, G., Taub, E., Morris, D., Vignolo, M., McCulloch, K., 2005. Reliability and validity of the upper-extremity motor activity Log-14 for measuring real-world arm use. Stroke 36, 2493–2496.

van den Heuvel, M.P., Mandl, R.C., Kahn, R.S., Hulshoff Pol, H.E., 2009. Functionally linked resting-state networks reflect the underlying structural connectivity architecture of the human brain. Hum. Brain Mapp. 30, 3127–3141.

Varela, F., Lachaux, J.P., Rodriguez, E., Martinerie, J., 2001. The brainweb: phase synchronization and large-scale integration. Nat. Rev. Neurosci. 2, 229–239.

Veroude, K., Norris, D.G., Shumskaya, E., Gullberg, M., Indefrey, P., 2010. Functional connectivity between brain regions involved in learning words of a new language. Brain Lang. 113, 21–27.

Vincent, J.L., Patel, G.H., Fox, M.D., Snyder, A.Z., Baker, J.T., Van Essen, D.C., Zempel, J.M., Snyder, L.H., Corbetta, M., Raichle, M.E., 2007. Intrinsic functional architecture in the anaesthetized monkey brain. Nature 447, 83–86.

Volz, L.J., Rehme, A.K., Michely, J., Nettekoven, C., Eickhoff, S.B., Fink, G.R., Grefkes, C., 2016. Shaping early reorganization of neural networks promotes motor function after stroke. Cereb. Cortex 26, 2882–2894.

von Stein, A., Sarnthein, J., 2000. Different frequencies for different scales of cortical integration: from local gamma to long range alpha/theta synchronization. Int. J. Psychophysiol. 38, 301–313.

Vukelic, M., Bauer, R., Naros, G., Naros, I., Braun, C., Gharabaghi, A., 2014. Lateralized alpha-band cortical networks regulate volitional modulation of beta-band sensorimotor oscillations. NeuroImage 87, 147–153.

Vukelic, M., Gharabaghi, A., 2015a. Oscillatory entrainment of the motor cortical network during motor imagery is modulated by the feedback modality. NeuroImage 111, 1–11.

Vukelic, M., Gharabaghi, A., 2015b. Self-regulation of circumscribed brain activity modulates spatially selective and frequency specific connectivity of distributed resting state networks. Front. Behav. Neurosci. 9, 181.

Westlake, K.P., Hinkley, L.B., Bucci, M., Guggisberg, A.G., Byl, N., Findlay, A.M., Henry,

R.G., Nagarajan, S.S., 2012. Resting state alpha-band functional connectivity and recovery after stroke. Exp. Neurol. 237, 160–169.

Yassi, N., Churilov, L., Campbell, B.C., Sharma, G., Bammer, R., Desmond, P.M., Parsons, M.W., Albers, G.W., Donnan, G.A., Davis, S.M., 2015. The association between lesion location and functional outcome after ischemic stroke. Int. J. Stroke 10, 1270–1276.

Zhang, J.T., Ma, S.S., Li, C.R., Liu, L., Xia, C.C., Lan, J., Wang, L.J., Liu, B., Yao, Y.W., Fang, X.Y., 2016. Craving behavioral intervention for internet gaming disorder: re-mediation of functional connectivity of the ventral striatum. Addict. Biol. 23, 337–346.